Phys. Status Solidi RRL 5, No. 10–11, 400–402 (2011) / DOI 10.1002/pssr.201105380

pss +++rapid research letters+++
www.pss-rapid.com

X-ray reciprocal space mapping study on semipolar InAlN films coherently grown on ZnO substrates

Tomofumi Kajima[1], Atsushi Kobayashi[*,2], Kazuma Shimomoto[2], Kohei Ueno[1], Tomoaki Fujii[2], Jitsuo Ohta[2], Hiroshi Fujioka[2,3], and Masaharu Oshima[1,3]

[1] Department of Applied Chemistry, The University of Tokyo, Tokyo 113-8656, Japan
[2] Institute of Industrial Science, The University of Tokyo, Tokyo 153-8505, Japan
[3] CREST, Japan Science and Technology Agency, Tokyo 102-0075, Japan

Received 2 August 2011, revised 25 August 2011, accepted 25 August 2011
Published online 30 August 2011

Keywords InAlN, ZnO, X-ray reciprocal space mapping, semipolar

[*] Corresponding author: e-mail akoba@iis.u-tokyo.ac.jp, Phone: +81 –3-5452-6344, Fax: +81 –3-5452-6343

We have grown semipolar InAlN films on nearly lattice-matched ZnO $(1\bar{1}01)$ substrates and investigated their structural properties. Symmetric and asymmetric reciprocal space-mapping measurements have revealed that semipolar InAlN films grow coherently on ZnO $(1\bar{1}01)$ at room temperature. The narrow width of the X-ray rocking curves and the suppression of tilting of semipolar films can be attributed to this coherency. This forms a striking contrast with the case of semipolar AlN films grown on ZnO. We calculated In composition and lattice strain in the semipolar InAlN films based on a model for the lattice distortion of semipolar wurtzite crystal, and found that $In_{0.26}Al_{0.74}N$ $(1\bar{1}01)$ grows on ZnO substrates with small lattice strains of less than 1%.

$In_xAl_{1-x}N$ has been considered to be one of the most promising materials for optical devices such as light emitting diodes, laser diodes, and solar cells [1–5] because its band gap covers the range from 0.65 for InN to 6.0 eV for AlN [6, 7]. Recently, optical devices fabricated with semipolar group III-nitrides have attracted considerable attention for their potential to improve device performance by the suppression of the detrimental effects caused by built-in fields [8]. The epitaxial growth of semipolar InAlN films has rarely been reported, mainly due to two major problems in obtaining films with high crystalline quality. The first problem is the phase separation of InAlN. This stems from the thermal instability of InAlN alloy crystals [9, 10]. To solve this problem, a growth technique that functions under highly thermodynamically non-equilibrium conditions is highly desirable. For example, low temperature growth meets the requirement. The other problem is the lack of appropriate substrates for growth of semipolar InAlN films. In order to obtain high-quality InAlN films, substrates that give precise alignment of the positions of atoms at the hetero-interface are required. ZnO substrates for the growth of semipolar InAlN films are attractive from this viewpoint, because InAlN and ZnO share the same crystalline structure (wurtzite) and their lattice mismatch is small. In addition, recent progress in the hydrothermal growth technique has made it possible to obtain high-quality ZnO single crystals with large diameters at low cost. Despite all of these advantages, interfacial reactions between III-nitrides and ZnO substrates at high temperature make it difficult to take advantage of ZnO substrates [11]. Recently, we have found that pulsed laser deposition (PLD) allows us to dramatically reduce the growth temperature for group III-nitrides, and also to use ZnO substrates [12–15]. In fact, we have demonstrated the epitaxial growth of polar [16] and nonpolar [17] InAlN films on ZnO substrates at room temperature (RT), and found that the PLD RT growth technique is effective in suppressing phase separation in InAlN films.

The optical and electrical properties of InAlN are strongly influenced by the compositional ratio and strain state of the film. However, there have been few reports on the structural characteristics of strained semipolar InAlN films, probably because the simultaneous determination of

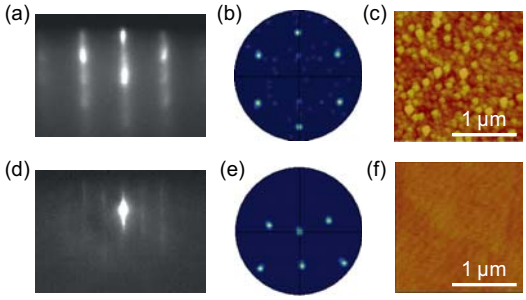

Figure 1 (online colour at: www.pss-rapid.com) RHEED patterns, {1 $\bar{1}$01} EBSD pole figures, and AFM imgages for InAlN films grown on ZnO (1 $\bar{1}$01) at (a)–(c) 550 °C, and (d)–(f) RT.

composition and strain in semipolar epitaxial films requires considerable effort. In this Letter, we report on the detailed structural characteristics of semipolar InAlN (1 $\bar{1}$01) films that have been coherently grown on ZnO (1 $\bar{1}$01) substrates at RT. We determined In composition and strain in semipolar InAlN by analysing the data from X-ray reciprocal space-mapping (RSM) for various diffractions.

We grew InAlN films on mechano-chemically polished ZnO (1 $\bar{1}$01) substrates. The ZnO (1 $\bar{1}$01) substrates were introduced into an ultra-high vacuum PLD chamber after surface cleaning with ethanol. A KrF excimer laser (wavelength 248 nm, pulse duration 20 ns) was used to alternately ablate an indium metal target and an AlN ceramic target during growth. The energy density of the excimer laser was 3.0 J/cm^2 and the pulse repetition rate was set to 20 Hz. For the nitrogen source, a radio-frequency plasma radical generator operating at 400 W with an N_2 pressure of 5.0×10^{-6} Torr was used. During the growth, the InAlN surfaces were monitored by reflection high-energy electron diffraction (RHEED). The structural characteristics of the semipolar InAlN films were investigated by electron backscattering diffraction (EBSD), atomic force microscopy (AFM) and high-resolution X-ray diffraction. The thicknesses of the InAlN films were measured with grazing-incidence X-ray reflection.

Two types of InAlN films were prepared on ZnO (1 $\bar{1}$01) substrates and compared. One is the 65 nm thick film grown at 550 °C, and the other is the 70 nm thick film grown at RT. The InAlN film grown at 550 °C exhibited a circular RHEED pattern during the initial stage of the growth. It eventually changed to the spotty pattern shown in Fig. 1(a). This is similar to that of RHEED patterns for *c*-plane InAlN films. The 70 nm thick InAlN film grown at RT exhibited the streaky RHEED pattern shown in Fig. 1(d) throughout the entire growth process. The pattern was similar to that for the ZnO (1 $\bar{1}$01) substrate. This indicates that a single-crystal InAlN (1 $\bar{1}$01) film with a flat surface has grown. We performed EBSD measurements in order to determine the crystallographic orientation of the InAlN surface. A {1 $\bar{1}$01} pole figure for the sample grown at 550 °C indicates the growth of a *c*-plane InAlN film with a small misorientation angle, as shown in Fig. 1(b). This misorientation phenomenon is probably caused by the interfacial reactions that occur between InAlN films and ZnO substrates at high growth temperature [16]. Figure 1(e) shows the {1 $\bar{1}$01} pole figure for the InAlN film grown at RT. The EBSD pole figure suggests that an InAlN (1 $\bar{1}$01) film has grown epitaxially on a ZnO (1 $\bar{1}$01) substrate, which is in good agreement with the RHEED observations. Figures 1(c) and 1(f) show AFM images of InAlN films grown on ZnO substrates at temperatures of 550 °C and RT, respectively. The surface of the film grown at 550 °C was rough and showed a root mean square (rms) value of 1.7 nm. We speculated that the degradation of the surface morphology of this sample was caused by an interfacial reaction that occurs during the growth of InAlN films on ZnO substrates. The film grown at RT exhibited a smooth surface with rms roughness of 0.27 nm. This is consistent with the streaky RHEED pattern shown in Fig. 1(d). We evaluated mosaicity of the InAlN films by measuring 1 $\bar{1}$01 X-ray rocking curves (XRC). The full-width at half-maximum values for the InAlN 1 $\bar{1}$01 XRC were 100 arcsec and 87 arcsec with the incident X-ray azimuths parallel to the *a*-axis and perpendicular to the *a*-axis, respectively.

We performed symmetric RSM measurements to investigate the crystallographic orientation relationship between semipolar InAlN and ZnO in detail. Figure 2 shows symmetric RSMs around the 1 $\bar{1}$01 diffraction with q_x parallel to [$\bar{1}$102] (a) and to [11$\bar{2}$0] (b) for the sample prepared at RT. In both Figs. 2(a) and 2(b), the reciprocal points for ZnO and InAlN were located at the same position in q_x, indicating that the (1 $\bar{1}$01) plane of the InAlN film was parallel to that of the ZnO substrate [18]. This confirmed that the film had grown coherently on the substrate [19]. This phenomenon is in striking contrast with the growth of a semipolar AlN film on a ZnO substrate [20].

We also performed asymmetric RSM measurements around the 2$\bar{2}$00 and 3 $\bar{1}\bar{2}$2 diffractions in order to determine In composition taking into account the stresses in semipolar InAlN films grown coherently on ZnO (1 $\bar{1}$01) substrates. The results are shown in Figs. 3(a) and 3(b), respectively. Although alloy composition in coherently-grown semipolar AlGaN and InGaN can be determined with only symmetric RSM measurements [21], here we performed additional asymmetric RSM measurements on

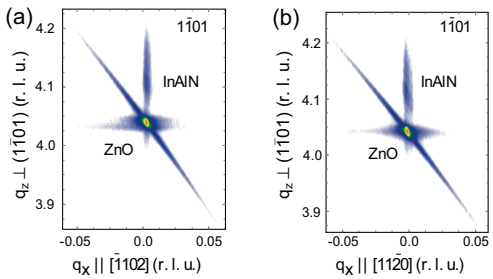

Figure 2 (online colour at: www.pss-rapid.com) Symmetric RSMs around 1 $\bar{1}$01 diffraction with X-ray incidence on (a) the plane containing the [1 $\bar{1}$01] and the [$\bar{1}$102] directions, and (b) the plane containing the [1 $\bar{1}$01] and the [11$\bar{2}$0] directions.

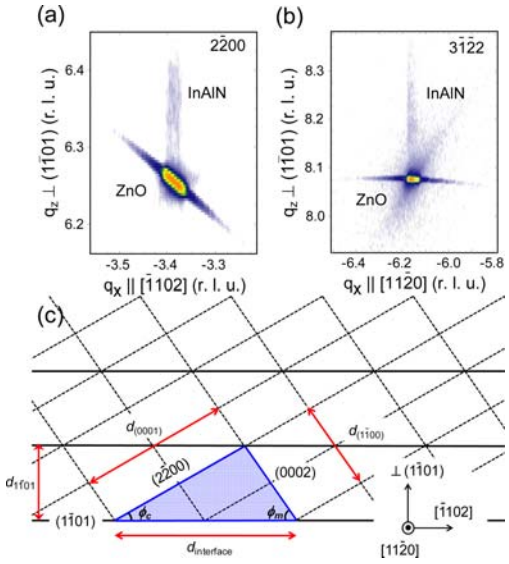

Figure 3 (online colour at: www.pss-rapid.com) Asymmetric RSMs for (a) $2\bar{2}00$ and (b) $3\bar{1}\bar{2}2$ diffractions for $In_{0.26}Al_{0.74}N$ $(1\bar{1}01)$. (c) Definition of plane intervals and angles.

semipolar InAlN to investigate their stress comprehensively. The intervals between the crystallographic planes obtained from the $2\bar{2}00$ RSM, $d_{(1\bar{1}00)}$ and $d_{interface}$, are 2.783 Å and 5.925 Å, respectively. The angle between the $(1\bar{1}00)$ and $(1\bar{1}01)$ planes, φ_m, is 61.9°. The plane intervals and angles are defined as shown in Fig. 3(c). The lattice parameter of the c-axis $[d_{(0001)}]$ can be calculated to be 5.228 Å by using these values and the law of cosines. The $3\bar{1}\bar{2}2$ RSM measurement has revealed that the lattice parameter a is 3.256 Å, and the spacing of the $(1\bar{1}01)$ planes $d_{(1\bar{1}00)}$ is 2.438 Å. Here, we assumed that the lattice constants of $In_xAl_{1-x}N$ follow Vegard's law and that the elastic constants can be determined by linear interpolation between the values for InN and AlN. We employed the model for the lattice deformation of semipolar nitride semiconductors as proposed by Funato et al. [18]. The model is consistent with the present phenomenon that the reciprocal points for the coherent InAlN and ZnO aligned vertically in asymmetric RSM. The lattice parameters and elastic constants for InN and AlN were cited from Refs. [22–25]. According to the rule of tensor component transformation, the relationship between the lattice strains can be represented by the following equation:

$$\varepsilon_{z'z'} = \varepsilon_{yy} \sin^2\theta + \varepsilon_{zz} \cos^2\theta + \varepsilon_{yz} \sin 2\theta\,, \qquad (1)$$

where ε_{yy}, ε_{zz}, and $\varepsilon_{z'z'}$ are the strains along $[1\bar{1}01]$, [0001], and the direction normal to the surface, respectively. ε_{yz} is the shear strain in the plane made by the c- and m-axes. θ represents the angle between the c-plane and the semipolar plane [62° for $(1\bar{1}01)$]. Because we assumed that the variables in Eq. (1) are dependent on In composition in InAlN, we can find the only set of values that satisfies the equation. Using this relationship, we found the values of In composition x = 0.26, ε_{xx} = 0.98% along the a-axis, ε_{yy} = –0.40% along the m-axis, ε_{zz} = 0.69% along the c-axis, and shear strain ε_{yz} = –0.75%. The critical thickness for the onset of stress relaxation was calculated according to Refs. [26, 27]. The value for InAlN $(1\bar{1}01)$ on ZnO was found to be about 16 nm. The thickness of the coherent InAlN in this study is greater than the theoretical value. The boost of critical thickness for stress relaxation may be attributed to a non-equilibrium growth condition with PLD.

In summary, we have succeeded in the epitaxial growth of high-quality semipolar InAlN $(1\bar{1}01)$ films on ZnO $(1\bar{1}01)$ substrates with the PLD RT growth technique. RSM measurements revealed that semipolar InAlN films grow on ZnO substrates without tilting of the surface normal direction due to suppression of the introduction of strain relaxation. We also calculated In composition and lattice strain in the semipolar InAlN films based on a model for the lattice distortion of semipolar wurtzite crystals, and we found that $In_{0.26}Al_{0.74}N$ $(1\bar{1}01)$ films grow on ZnO substrates with low lattice strains of less than 1%, which allows the possibility of coherent growth. These results indicate that ZnO substrates in combination with the PLD RT-growth technique were promising for the fabrication of semipolar InAlN-based optoelectronic devices.

Acknowledgements This work was partially supported by the "R&D on Innovative PV Power Generation Technology" project, contracted by The University of Tokyo with New Energy and Industrial Technology Development Organization (NEDO).

References

[1] S. Yamaguchi et al., Appl. Phys. Lett. **76**, 876 (2000).
[2] W. Terashima et al., Jpn. J. Appl. Phys. **45**, L539 (2006).
[3] Y. Houchin et al., Phys. Status Solidi C **5**, 1571 (2008).
[4] E. Iliopoulos et al., Appl. Phys. Lett. **92**, 191907 (2008).
[5] R. E. Jones et al., J. Appl. Phys. **104**, 123501 (2008).
[6] C. S. Gallinat et al., Appl. Phys. Lett. **89**, 032109 (2006).
[7] Y. Taniyasu et al., Nature **441**, 325 (2006).
[8] J. S. Speck and S. F. Chichibu, MRS Bull. **34**, 304 (2009).
[9] T. Matsuoka, Appl. Phys. Lett. **71**, 105 (1997).
[10] A. Koukitu and H. Seki, Jpn. J. Appl. Phys. **353**, L1638 (1996).
[11] A. Kobayashi et al., Appl. Phys. Lett. **88**, 181907 (2006).
[12] J. Ohta et al., Appl. Phys. Lett. **81**, 2373 (2002).
[13] J. Ohta et al., Appl. Phys. Lett. **83**, 3060 (2003).
[14] Y. Kawaguchi et al., Appl. Phys. Lett. **87**, 221907 (2005).
[15] M. H. Kim et al., Appl. Phys. Lett. **89**, 031916 (2006).
[16] T. Kajima et al., Appl. Phys. Express **3**, 021001 (2010).
[17] T. Kajima et al., Jpn. J. Appl. Phys. **49**, 070202 (2010).
[18] M. Funato et al., J. Appl. Phys. **107**, 123501 (2010).
[19] A. Kobayashi et al., Phys. Status Solidi A **208**, 834 (2011).
[20] K. Ueno et al., Phys. Status Solidi RRL **3**, 58 (2009).
[21] E. C. Young et al., Appl. Phys. Express **4**, 073512 (2011).
[22] X. Wang et al., J. Appl. Phys. **99**, 073512 (2006).
[23] A. F. Wright, J. Appl. Phys. **82**, 2833 (1997).
[24] F. A. Ponce et al., Appl. Phys. Lett. **67**, 410 (1995).
[25] K. Tsubouchi and N. Mikoshiba, IEEE Trans. Sonics Ultrason. **32**, 634 (1985).
[26] E. C. Young et al., Appl. Phys. Express **3**, 111002 (2010).
[27] A. E. Romanov et al., J. Appl. Phys. **109**, 103552 (2011).

